Experimental analysis of jet slurry erosion on martensitic stainless steel

IOP Conf. Series: Materials Science and Engineering **659** (2019) 012077 doi:10.1088/1757-899X/659/1/012077

Experimental analysis of jet slurry erosion on martensitic stainless steel

G Santacruz[1], A S Takimi[1], F Vannucchi de Camargo[1,2], C P Bergmann[1]

[1] Post-Graduation Program in Mining, Metallurgical and Materials Engineering, Federal University of Rio Grande do Sul - UFRGS, Osvaldo Aranha 99, Porto Alegre, RS 90035-190, Brazil
[2] Department of Industrial Engineering, University of Bologna, Viale del Risorgimento 2, 40136, Bologna, Italy

E-mail: galileo.santacruz@ufrgs.br

Abstract. Due to their enhanced tribological properties that contribute to an increased useful life of components, martensitic stainless steels are an excellent option for industrial applications such as hydroelectric, petrochemical, civil construction and mineral processing plants. In the present investigation, the erosive wear of AISI 410 martensitic stainless steel is evaluated after thermal treatment by quenching and tempering by mass loss, under erosive attack at 30◦ and 90◦ incidence angles, using a self-made jet slurry erosion equipment controlling parameters such as speed, volume of fluid, temperature and concentration of erosive particles of erodent. The characterization of the eroded samples was carried out in terms of the microstructure (SEM) and microhardness as well as the particle size distribution (LG) and morphology of the erodent. It was possible to establish the relationship between the slurry erosive wear and the physical properties inherent of stainless steel for this particular experimental configuration, concluding that the steel presents better resistance to jet slurry erosion wear when compared to austenitic steel commonly used in the industry.

1. Introduction

In different industrial applications, such as hydraulic turbines in hydroelectric plants, petrochemical industry, construction, and in the processing of minerals, the loss of metal due to slurry erosion caused by the particulate material in the liquid represents a major industrial problem affecting the life of the components and reducing their performance. Thus, the ideal choice of engineering materials is important in order to decrease the wear rate and to improve their tribological behavior. Among the different alternatives for such applications, the most current being studied is the austenitic and martensitic stainless steels. Austenitic stainless steels are used in many components where corrosion resistance is crucial. However, under the mechanical action of hard particles, they present a high plastic deformation and wear [1]. On the other hand, martensitic stainless steel presents better mechanical resistance to erosive particles than austenitic steel, with the compromise of a lower corrosion resistance [2-5].

In the present investigation, it was possible to evaluate the erosive wear of the martensitic stainless steel AISI 410 thermally treated with quenching and tempering, evaluating the volume loss under jet slurry erosion conditions at incidence angles of 30° and 90° between the axis of symmetry of the fluid

flow and the surface of the samples, via the control of parameters such as angle and speed of impact, test temperature and concentration of erosive particles in the suspension. In this case, electrofused alumina was used as erodent.

The materials were characterized with regard to their microstructure by scanning electron microscopy (SEM), roughness, microhardness, and the particle size distribution analyzed with laser granulometry (LG) and morphology of the erodent.

2. Materials and Methods

2.1. Martensitic stainless steel AISI 410

AISI 410 martensitic stainless steel cylindric coupons with 30 mm in diameter and 10 mm in height were used. The chemical composition of the steel is presented in Table 1. The steel samples were tempered at 1263 K for 35 min then oil-quenched at 793 K for another 35 min. The microstructure obtained after this procedure was composed of martensite with its grain contours and some precipitated carbides, typical of quenching and tempering thermal treatments presented in Figure 1.

Table 1. Chemical composition of the AISI 410 martensitic stainless steel used in this investigation (wt.%).

Elements	Composition (%)
C	0.020
Cr	11.200
Mn	0.590
Si	0.720
Ni	0.350
P	0.022
S	0.002
N	0.021

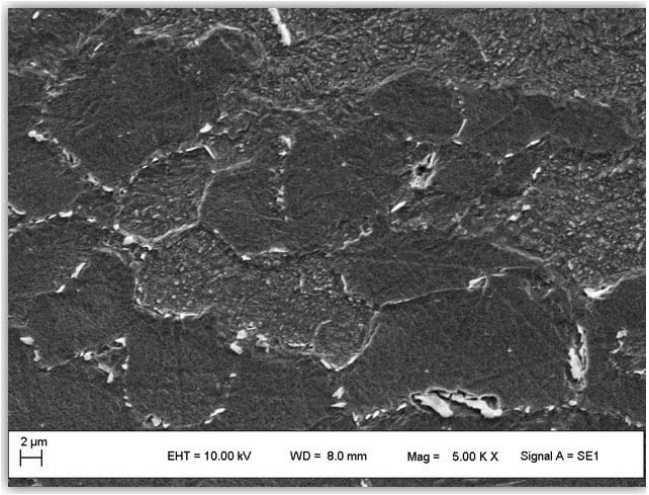

Figure 1. Microstructure of AISI 410 stainless steel quenched and tempered. (SEM 5000x, Vilella's acid etching).

2.2. Erodent particles

Cilas 1180 laser diffraction particle size analyzer was used to measure the particle size distribution of the alumina erodent (Al_2O_3). The technique follows the ISO 13320:2009 standard [6]. The abrasive

particle size distribution is shown in Figure 2, yielding an average abrasive particle size of about 98.55 μm. SEM micrograph shows angular and irregularly shaped particles in Figure 3.

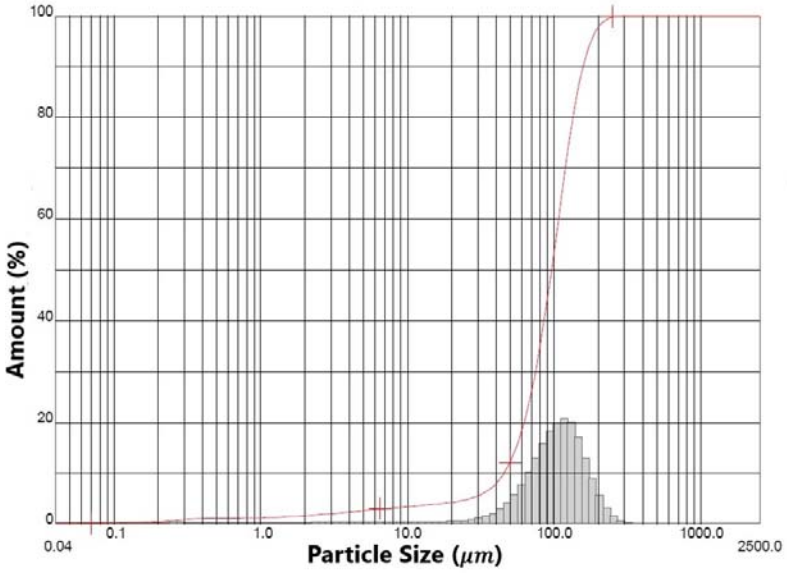

Figure 2. Particle size distribution of aluminum oxide.

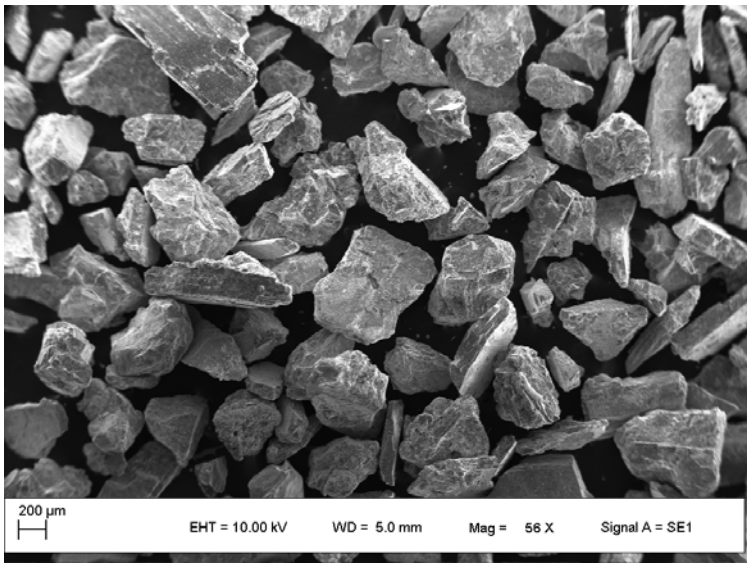

Figure 3. SEM micrograph showing the abrasive particles shape and size. (56x).

2.3. Microstructure characterization

The microstructure characterization was done in an EVO MA10 SEM and an optical microscopy LEICA DM2700 M. Surface roughness of the steel samples was measured before the jet slurry erosion and after it using a surface roughness tester Mitutoyo SJ-400. Then, cross-sectional Vickers microhardness measurements were performed by using a Buehler Micromet 2001 microhardness tester (HV300 g, 30 s) following ASTM E-384-11 standard [7].

2.4. Jet Slurry erosion tests

The jet slurry erosion tests were carried out in a modified commercial high pressure washer which is based on ASTM G-76 standard [8-12] and adapted in the nozzle of the gun a system of feeding of erodent particles using an inner Venturi accelerator of particles inside a test chamber. This equipment allows controlling the angle of impact, the speed of impact, the concentration of erosive particles in the suspension and test temperature, all important parameters to determine the distribution of frictional energy along a surface [13]. Figure 4 shows the configuration of the testing device.

The tests were performed using water between 25 and 28°C of temperature with 960 g of (Al_2O_3) erodent. The samples were placed at the nozzle output to guarantee the incidence of impact fluid and mean jet velocity of erosive material in the suspension of 77 m/s. This velocity was calculated using flow rate, time and nozzle area measurements of flow output. The incidence angles studied were 30° and 90° between the axis of symmetry of the fluid flow and the surface of the samples. In all cases, the concentration of particles in the slurry was 7 wt% [14-16]. The erosion resistance was determined from the volume loss results per unit of time from the difference of mass loss considering the relation of the apparent density of the studied material (7.73 g/cm^3 for AISI 410 stainless steel [17-19]). Mass losses were measured every 1 min by using a scale with 0.01 mg resolution. The total duration of each test was 4 min. The samples were cleaned in an ultrasonic bath with deionized water before and after each test and dried and weighted afterwards.

3. Results and Discussion

3.1. Mechanical Properties of Materials

Microhardness reflects the microstructure and the physical and mechanical properties of both substrate and coating, which in turn are dependent on the materials and processes employed in their manufacture. Hardness is a property that can be considered variable throughout the material in certain zones due to eventual heterogeneities of the material. For this reason, when measuring this property, one must consider the preparation of the surface, the section analyzed, as well as the number of indentations performed. The microhardness of AISI 410 is presented in Table 2.

Figure 5 shows the indentation performed on the thermally treated martensitic AISI 410 stainless steel. The measured microhardness value was 219 HV0.3, which is very similar to that reported by [16] of 199 HV0.3.

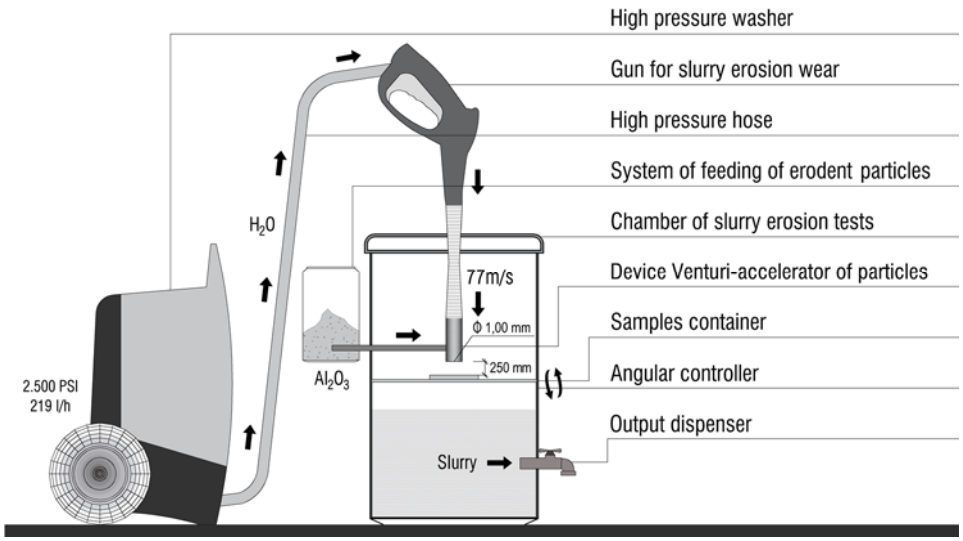

Figure 4. Schematic diagram of the jet slurry erosion tester.

Table 2. Results of Vickers microhardness measurements - cross section (HV0.3 - 2.94N)

Microhardness (HV)	
Average	219.30
Standard Deviation	±31.07
Coefficient of Variation (%)	14.16

Table 3 shows the accumulated erosion rate by mass of erodent impacted in loss of volume of the samples tested, as a function of the impact angle, in a total time of 4 minutes, for the samples used in the research of stainless steel AISI 410 martensitic.

Table 3. Accumulated erosion rate after 4 minutes.

Material	Impact Angle (°)	Volumetric Erosion Rate $(cm^3_{target}/g_{erodent})*10^{-5}$	Standard Deviation $(cm^3_{target}/g_{erodent})*10^{-5}$
Steel AISI 410	30	0.8449	±0.0114
	90	0.7025	±0.0495

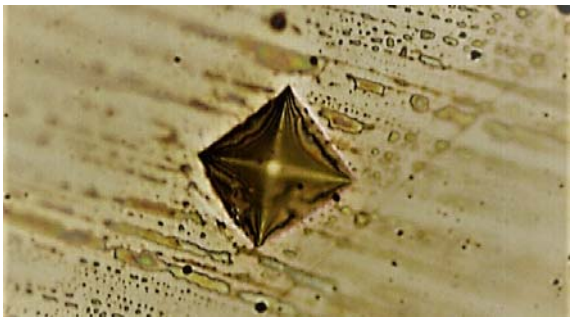

Figure 5. Vickers indentation (219 HV0.3) performed for thermally treated AISI 410 martensitic stainless steel. (OM, 50x).

Figure 6 shows the average mass losses measured in 3 samples every 1 min until a total erosion time of 4 minutes for the impact angles of 30° and 90°. Steel exhibits a much higher erosive wear at 30° impact angle than at 90°, demonstrating a ductile behavior with a ploughing-predominant material removal mechanism, as reported in the literature [20,21]. Furthermore, many authors confirm that metals present an enhanced erosion rate at lower angles [22-25]. Figure 6 also shows that, for the impact angle of 90°, the samples presented an accumulated volumetric erosion rate slightly lower than the 30° impact angle.

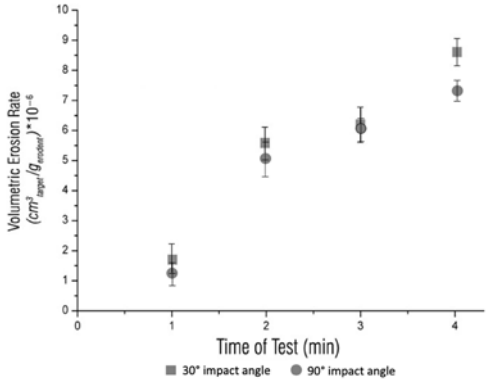

Figure 6. Variation of the accumulated volumetric erosion rate as a function of the impact angle of for AISI 410.

Figure 7 shows the areas of the erosion regions of the samples subjected to the jet slurry erosion test for the impact angles of 30° and 90°. It is observed that the eroded region of the pieces (highlighted in red) tested with the angle of 30° have an elongated shape and greater erosion area. The erosion of the pieces tested in the angle of 90° is more localized, has a smaller area and a greater depth. In the samples, it is possible to notice the formation of a concentric ring, described as "halo erosion" in the literature, which is a mechanical characteristic of the damage due to the development of craters that appear as macro pits on the surface for this angle [26-28]. The eroded region roughness in the samples, for the two impact angles, as shown in Table 4. Table 5 shows the areas of eroded regions according to the impact angle. It is observed that the eroded area is greater for the impact angle of 30°.

Table 4. Result of the average roughness measurement before and after jet slurry erosion.

Roughness					
Material	Before Erosion (μm)	Standard Deviation (μm)	Angle (°)	After Erosion (μm)	Standard Deviation (μm)
Steel AISI 410	0.07	±0.03	30	2.97	±0.47
			90	2.56	±0.11

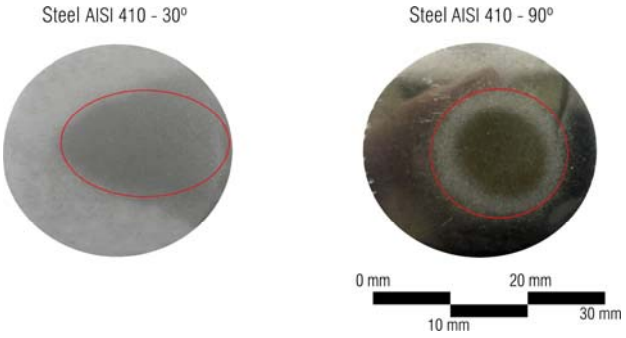

Figure 7. Areas of the eroded regions of the materials submitted to the jet slurry erosion test.

Table 5. Eroded area as a function of the impact angle.

Material	Impact angle (°)	Eroded area (mm^2)
Steel AISI 410	30	277.7
	90	147.1

Figure 8 shows the three-dimensional scanning of the samples submitted to the jet slurry erosion test obtained through the Geomagic Studio software, for impact angles of 30° and 90°, with which it was possible to estimate the average of the erosion depth (Table 6). As result, the average erosion depth of the samples tested at 90° is higher and more localized in relation to the samples tested at 30°.

Figure 8. Three-dimensional scanning of the samples submitted to the jet slurry erosion test.

Table 6. Average depth of the eroded regions.

Material	Impact angle (°)	Average depth (μm)	Standard Deviation (μm)
Steel AISI 410	30	93	±2.88
	90	102	± 15.87

The erosion study [20] conducted in steel tubes, varying impact angle and velocity, also found out that at a 90° angle, deeper eroded areas are found in comparison to samples tested at 30°, agreeing with the results presented in Table 6. Similarly, studies [28] have investigated the performance of the AISI 420 stainless steel subjected to particle erosion tests using two different abrasives at the angles of incidence of 30°, 45°, 60° and 90°. The results also showed that the samples evaluated at 90° presented a greater depth profile than those at 30° even when two different abrasives are adopted, obtaining 450 and 929 *nm* for the angle of 90°, and 180 and 400 *nm* for the angle of 30°, respectively.

Furthermore, it is possible to verify that large erosion rates at smaller impact angles are an intrinsic feature of metals, whereas in the case of brittle ceramics, for instance, higher erosion rates are identified in angles closer to 90° [29]. For this reason, ceramic coatings are an alternative to improve the erosion resistance of metallic materials [30, 31].

4. Conclusion

In the present investigation, completing provisional results from similar researches [32], the jet slurry erosion behavior of martensitic stainless steel AISI 410 was investigated. From the results obtained in the accomplishment of the experimental work, it is possible to infer the following conclusions:

- An experimental erosion wear simulation equipment of the jet slurry type was developed, considering conditions that allowed the control of the test parameters such as impact angle, impact velocity, erosive particle concentration in the suspension and test temperature, all significant variables in the determination of the behavior of the materials.
- The AISI 410 martensitic stainless steel presented a higher rate of accumulated volumetric erosion in the impact angle of 30°, presenting a predominantly ductile behavior, and a higher resistance to jet slurry erosion at the impact angle of 90° with the compromise of deeper eroded area.

Acknowledgment

The authors express their gratitude to the following laboratories: Laboratory of Ceramic Materials (LACER), Laboratory of Physical Metallurgy (LAMEF), Laboratory of Design and Selection of Materials (LdSM) and the Laboratory of Conventional Machining (LUC) of the Federal University of Rio Grande do Sul (UFRGS) for the investigation support and to the Research and Technology Center of Rijeza Metallurgy. G. Santacruz and F.V. de Camargo thank the Coordination of Improvement of Higher Education Personnel of the Brazilian Ministry of Education (CAPES/MEC) for the doctorate scholarship grants 88882.345871/2019-01 and 88882.345831/2019-01, respectively.

References

[1] Toro A, Sinatora A, Tanaka D K and Tschiptschin A P 2001 Corrosion–erosion of nitrogen bearing martensitic stainless steels in seawater–quartz slurry, *Wear* **251**(1) 1257–1264
[2] Levy A V and Yau P 1984 Erosion of steels in liquid slurries, *Wear* **98** 163–182
[3] Guaglianoni W C, Cunha M A, Bergmann C P, Fragassa C and Pavlovic A 2018 Synthesis, Characterization and Application by HVOF of a WCCoCr/NiCr Nanocomposite as Protective Coating Against Erosive Wear, *Tribology in Industry* **40(**3) 477-487
[4] Mesa D H, Toro A, Sinatora A and Tschiptschin A P 2003 The effect of testing temperature on corrosion–erosion resistance of martensitic stainless steels, *Wear* **255**(1-6) 139-145

[5] Babic M, Calì M, Nazarenko I et al. 2018 Surface Roughness Evaluation in Hardened Materials by Pattern Recognition Using Network Theory, *International Journal on Interactive Design and Manufacturing* **13**(1) 211-219
[6] BS ISO 13320 2009 *Particle Size Analysis-Laser Diffraction Methods*.
[7] ASTM E384 2011 *Standard Test Method for Knoop and Vickers Hardness of Materials*.
[8] ASTM G76 2013 *Standard Test Method for Conducting Erosion Tests by Solid Particle Impingement using Gas Jets*.
[9] Zu J B, Hutchings I M and Burstein G T 1990 Design of a slurry erosion test rig, *Wear* **140**(2) 331–344
[10] Wentzel E J and Allen C 1997 The erosion-corrosion resistance of tungsten-carbide hard metals, *Int J Refractory Met Hard Mat* **15**(1-3) 81–87
[11] Santa J F, Baena J C and Toro A 2007 Slurry erosion of thermal spray coatings and stainless steels for hydraulic machinery, *Wear* **263**(1) 258–264
[12] Santa J F, Espitia L A, Blanco J A, Romo S A and Toro A 2009 Slurry and cavitation erosion resistance of thermal spray coatings, *Wear* **267**(1) 160–167
[13] Willert E 2019 Energy Loss and Wear in Spherical Oblique Elastic Impacts, *Facta Universitatis, Series: Mech Eng* **17**(1) 75-85
[14] Hutchings I M 1981 A model for the erosion of metals by spherical particles at normal incidence, *Wear* **70**(3) 269– 281
[15] Finnie I 1995 Some reflections on the past and future of erosion, *Wear* **186** 1–10
[16] Maiti A K, Mukhopadhyay N and Raman R 2009 Improving the wear behavior of wc-cocr-based hvof coating by surface grinding, *J Mat Eng Performance* **18**(8) 1060
[17] Madsen B W 1988 Measurement of erosion-corrosion synergism with a slurry wear test apparatus, *Wear* **123**(2) 127–142
[18] Murthy J K N, Rao D S and Venkataraman B 2001 Effect of grinding on the erosion behaviour of a wc–co–cr coating deposited by hvof and detonation gun spray processes, *Wear* **249**(7) 592–600
[19] Liu X and Zhang B 2002 Effects of grinding process on residual stresses in nanostructured ceramic coatings, *J Mat Sci* **37**(15) 3229–3239
[20] Islam M D A and Farhat Z N 2014 Effect of impact angle and velocity on erosion of api x42 pipeline steel under high abrasive feed rate, *Wear* **311**(1-2) 180–190
[21] Okonkwo P C, Shakoor R A, Zagho M M and Mohamed A M A 2016 Erosion behaviour of api x100 pipeline steel at various impact angles and particle speeds. *Metals* **6**(10) 232
[22] Bayer R G 1994 Mechanical wear prediction and prevention, *Marcel! Dekker, Inc, P. O. Box 5005, Monticello, NY 12701-5185, USA, 1994. 657*
[23] Papini M and Spelt J K 1998 The plowing erosion of organic coatings by spherical particles, *Wear* **222**(1) 38–48
[24] O'Flynn D J, Bingley M S, Bradley M S A and Burnett A J 2001 A model to predict the solid particle erosion rate of metals and its assessment using heat-treated steels, *Wear* **248**(1-2) 162–177
[25] Biswas A, Satapathy A and Patnaik A 2010 Erosion wear behavior of polymer composites: a review, *J Reinf Plastics Composites* **29**(19) 2898–2924
[26] Wood F W 1986 Erosion by solid-particle impacts: a testing update, *J Testing and Evaluation* **14**(1) 23–27
[27] Souza V A and Neville A 2003 Corrosion and erosion damage mechanisms during erosion–corrosion of wc–co–cr cermet coatings, *Wear* **255**(1-6) 146–156
[28] Vite-Torres M, Laguna-Camacho J R, Baldenebro-Castillo R E, Gallardo-Hernandez E A, Vera-Cárdenas E E and Vite-Torres J 2013 Study of solid particle erosion on aisi 420 stainless steel using angular silicon carbide and steel round grit particles, *Wear* **301**(1-

2) 383–389
[29] Dauber C, de Camargo F V, Alves A K, Pavlovic A, Fragassa C and Bergmann C P 2019 Erosion Resistance of Engineering Ceramics and Comparative Assessment through Wiederhorn and Evans Equations, *Wear* **432-433**:202938. DOI: 10.1016/j.wear.2019.202938
[30] Cunha M A, Guaglianoni W C, Bezerra B F A, de Camargo F V and Bergmann C P 2019 Resistance to Abrasive and Erosive Wear of WCCo/NiCr HVOF Coatings: Comparative Evaluation of Commercial Nanostructured Spray Powders. *Tribology in Ind*, In press
[31] Campione I., Fragassa C, Martini A 2019 Kinematics optimization of the polishing process of large-sized ceramic slabs, *International Journal of Advanced Manufacturing Technology* **103** (1-4), 1325-1336. doi: 10.1007/s00170-019-03623-3.
[32] Santacruz G, Takimi A, Vannucchi de Camargo F, Bergmann CP, Fragassa C. 2019 Comparative Study of Jet Slurry Erosion of Martensitic Stainless Steel with Tungsten Carbide HVOF Coating. *Metals* **9**(5), 600; doi:10.3390/met9050600.